

Hydrodynamic planetary thermosphere model. II: coupling of energetic electron transport model (draft)

Feng Tian, Stan C. Solomon, Liying Qian, Jiuhou Lei, James F. Kasting, Ray G. Roble

1. Introduction

In a previous paper (Tian, Kasting, Liu, and Roble 2007, hereafter Paper I), the first 1-D, multi-component, hydrodynamic model (hereafter model I) has been developed to investigate the response of the thermosphere/ionosphere of a hypothetical Earth-like planet to extreme solar EUV inputs. The chemical scheme in model I is generalized from theoretical models of planetary atmospheres (Earth, Venus, Mars, and giant planets) and the hydrostatic equilibrium assumption has been relieved from the dynamic consideration in order to correctly characterize the hydrodynamic nature of planetary thermospheres under extremely strong solar EUV conditions. Despite these advances, model I still relies on parameterizations developed in the present Earth's thermosphere in the following aspects: 1) ionizations, excitations, and dissociations by electron impact processes; 2) heating of ambient electrons by photoelectrons and secondary electrons. In order to treat both aspects correctly, an energetic electron transport model is needed. In this paper we couple an existing energetic electron transport model (the GLOW model) with model I and investigate the behavior of the thermosphere as well as various photon and electron impact processes in the thermosphere under extreme EUV conditions. For simplicity, the atmospheric composition at the lower boundary (~97 km) is assumed to be the same as that present Earth.

The GLOW model contained three major species: O, O₂, and N₂. Because model I showed that atomic nitrogen can become dominant in the upper thermosphere under large solar EUV conditions, in this work we expand the GLOW model to include the photon and electron impact processes of N.

In Paper I, we discussed the importance of adiabatic cooling, associated with the hydrodynamic flow of one single background fluid including both neutral and ion species, to the neutral gas energy budget. Since quasi-neutrality is assumed in model I, electrons should be moving together with ions at the same velocity, if not greater. Thus the adiabatic cooling associated with the bulk motion of electrons could be an important cooling mechanism for electron gas. In this paper we solve the complete electron energy equation to address this issue.

2. Model descriptions and validations

2.1 model descriptions

The GLOW model is an energetic electron transport model developed for the Earth's thermosphere (Solomon et al. 1988, Bailey et al. 2002). A version of it has been applied to Venus (Alexander et al. 1993). We use the Earth version as the base for the expansion. For details of the GLOW model, readers are referred to Solomon, Bailey papers. The following is a brief description.

The GLOW model treats the transport of energetic electrons (photoelectrons, secondary electrons, and precipitated electrons) using a two-stream approach following Nagy and Banks (1970). Collisions between energetic electrons with ambient electrons and neutral gases are included. Elastic collisions influence the energetic electron fluxes (both upward and downward) directly while inelastic collisions (ionization, excitation, and dissociation) lead to the cascade of energetic electrons to less energetic electrons. Energetic electrons are divided into energy bins and the transport equation is solved for the highest energy bin first and the lowest energy bin last to fully account for the cascade processes. The GLOW model has been used to analyze and explain the observed O¹D airglow emissions in the Earth's thermosphere (Solomon and Abreu 1989). Parameterization methods (for the contributions to ionization, excitation, and dissociation by electron impact processes) developed based on the GLOW model have been employed by general circulation models such as TIE-GCM (Solomon and Qian 2005, and other [references](#)).

In this work, the electron impact ionization and excitation of N atoms is added in the GLOW model so that the model can be applied to extreme solar EUV conditions. Photoionization and absorption cross sections of N are from Fennelly and Torr (1992). For electron impact ionization, the cross sections in Avakyan et al. (1998) are used. The analytical expressions of Jackman et al. (1977) are used to fit the data and calculate the secondary electron distributions. For electron impact excitation, we include the following excited states into consideration: N2D0, N2P0, N3s4P, N2p44P, and N3s2P. The cross sections of the first 4 excited states are taken from Tayal et al. (2005) and fitted with the analytical expression in Green and Stolarski (1972). For the cross sections of N4S0->N3s2P, we use the cross sections in Stone and Zipf (1973), which is from emission measurements. Because the Lyman alpha calibration standard changed after the measurements were taken, the electron impact excitation cross sections of O atoms from the same authors need to be adjusted downward by as much as a factor of 2.8 (Zipf and Erdman 1985). Similar adjustments have not been reported for N atoms. The calculated peak cross sections in Tayal et al. (2005) for N4S-> N3s4P and N4S -> N2p44P are smaller than those reported in Stone and Zipf (1973) by about a factor of 4.5 and 5.2. Because the emission measurements include the contribution of cascade from other excited states, we take the freedom to adjust the cross section in Stone and Zipf (1973) downward by a factor of 2.8. Because the cross sections in Stone and Zipf (1973) is for the emission line of 1744A, they need to be multiplied by 2.79 to obtain the electron impact cross sections of N4S->N3s2P (Meier 1991). Through experiments, we obtained the fitting parameters for electron impact ionization and excitation of N summarized in Table 1 and 2.

Table 1. parameters for the electron impact ionization of N

I	K	J	Ts	Ta	Tb	Γs	Γb
14.55	2.49	3.62	7.05	3450	178	19.5	-0.815

Table 2. parameters for the electron impact excitation of N

Excited States	W	A	Ω	γ	v
² D	2.386	0.0540	1.35	1.00	1.60
² P	3.576	0.0325	1.48	0.60	1.04
3s ⁴ P	10.330	0.4124	0.69	1.02	2.00
3s ² P	10.687	0.1654	1.90	1.01	1.08
2p ⁴ P	10.924	0.1470	0.70	4.19	5.57

Note that these fitting parameters may have errors because 1) the fittings are not perfect and 2) electron impact excitation cross sections are read from figures in the corresponding references. A better approach would be to use cross section tables instead of fitting parameters, which will be useful future work. Elastic collisional cross sections and backscattering probabilities (both elastic and inelastic) of N are assumed to be the same as those of O. Auger ionization effect is ignored for N.

For electron gas energy equation, we start from that given in Schunk and Nagy (2000):

$$\frac{3}{2}n_e k \frac{\partial T_e}{\partial t} = -n_e k T_e \nabla \cdot \vec{u}_e - \frac{3}{2}n_e k \vec{u}_e \cdot \nabla T_e - \nabla \cdot \vec{q}_e + \sum Q_e - \sum L_e - \sum_i \frac{\rho_e v_{ei}}{m_i} 3k(T_e - T_i) - \sum_n \frac{\rho_e v_{en}}{m_n} 3k(T_e - T_n) \quad (1)$$

here k is the Boltzmann constant, n_e is the electron density, T_e is the electron temperature, u_e is the bulk motion velocity of the electron gas, q_e is the heat flux, $\sum Q_e$ is the sum of the external heating rates, $\sum L_e$ is the sum of the inelastic cooling rates. The last two terms on the right hand side are the elastic collisional cooling of electron gas by ions and neutrals.

In 1-D case, equation (1) can be simplified to the following format:

$$\frac{3}{2}n_e k \frac{\partial T_e}{\partial t} = -n_e k T_e \frac{\partial(u_e r^2)}{r^2 \partial r} - \frac{3}{2}n_e k u_e \frac{\partial T_e}{\partial r} + \frac{\partial}{\partial r} (\lambda_e r^2 \frac{\partial T_e}{\partial r}) + \sum Q_e - \sum L_e - \sum_i \frac{\rho_e v_{ei}}{m_i} 3k(T_e - T_i) - \sum_n \frac{\rho_e v_{en}}{m_n} 3k(T_e - T_n) \quad (2)$$

here r is the distance from the center of the planet, $\lambda_e = 7.7 \times 10^5 T_e^{5/2} eV \cdot cm^{-1} \cdot s^{-1} \cdot K^{-1}$ is the thermal conductivity. We ignored the angle between the magnetic field lines and the vertical direction in equation (2).

The first two terms on the right hand side of equation (2) are the adiabatic expansion and the advection cooling terms. In this paper we refer the sum of the two terms as adiabatic

cooling. The adiabatic cooling terms are normally negligible in the terrestrial ionosphere (Schunk and Nagy 2000) and are ignored in Paper I. However, because Paper I showed that the adiabatic cooling associated with the hydrodynamic flow can become the dominant cooling mechanism under extreme solar EUV conditions, the significance of adiabatic cooling to the electron gas in similar situations needs to be investigated. In this work Eq (2) is solved by assuming that the bulk motion velocity of electrons is the same as that of neutral and ion gases.

2.2 model validations

The profiles of temperature (neutral, ion, and electron), mass density, and number densities of various species (both ion and neutral) of the Earth's thermosphere under solar maximum and minimum conditions in this paper are similar to those in Paper I and will not be repeated here. Solomon and Qian (2005) presented the ionization and dissociation rate profiles for O, O₂, and N₂ in Earth's thermosphere under solar minimum condition (F107=70) for both low (0°) and high (85°) solar zenith angle conditions. Fig. 2.1 shows the profiles of photoionization, photodissociation, electron impact dissociation, and photoelectron enhancement factors calculated in the coupled model under solar minimum condition. The solar zenith angle is 60° and the dip angle (between the magnetic field and the vertical direction) is 22.7°. Our results are in good agreement with those in Solomon and Qian (2005). It is interesting to note that although electron impact can make significant contribution to the dissociation of N₂, its contribution to the total dissociation of O₂ is negligible because of the efficient dissociation of O₂ by the Schumann-Rouge Continuum.

4. Thermosphere and ionosphere under extreme solar EUV conditions

Fig. 4.1 shows the temperature profiles of the Earth's thermosphere under different solar EUV conditions. The profiles' shapes are similar to those in Paper I. Paper I showed that the Earth's thermosphere experienced a transition from a hydrostatic equilibrium regime into a hydrodynamic regime, in which the adiabatic cooling associated with the hydrodynamic flow becomes the dominant cooling mechanism in the upper thermosphere. A similar transition is found in this work. Paper I found that the transition from hydrostatic equilibrium regime to hydrodynamic regime starts when solar EUV flux reaches around 5x present EUV. The thermospheric temperature structures in this work are notably warmer than their counterparts in Paper I. In Fig. 4.2 we compare the exobase temperatures under different solar EUV conditions in this work with those in Paper I. It is apparent that the adiabatic cooling starts to take effect under weaker EUV energy fluxes (~4x present EUV) in this model. The comparison suggests that neutral gases heating in the present model is more efficient than that in Paper I. The possible causes will be discussed in the following section.

Fig 4.3 shows the neutral gas heating rate and the contributions of different channels in P=700 (4.6x present EUV) case. The profiles in P=700 case can be seen as typical profiles for all extreme solar EUV condition cases. Similar to the neutral gas heating profiles in present Earth's thermosphere (Roble et al. 1987, Roble 1995), the neutral gas

heating in upper thermosphere is dominated by the elastic collisions between electrons, ions, and neutrals (q_{en}). In the lower thermosphere the neutral gas heating is dominated by exothermic chemical reactions (q_{chem}) with UV heating (including SRC, SRB, Lyman alpha, and various bands of O₂ and O₃) as a complimentary heating source. Joule heating is unimportant in all altitudes. Joule heating is included in the model by specifying an externally applied electric field (assumed constant with height) and calculating the Pedersen conductivity, similar to the treatment in the global mean model (Roble et al. 1987, Roble 1995). Because the Pedersen conductivity increases and the atmosphere expand with increasing solar EUV energy input, the Joule heating contribution increases in magnitude. Whether or not this parameterization can be applicable to the much more expanded thermosphere/ionosphere of the Earth under extreme solar EUV conditions needs future investigations.

Fig. 4.5 shows the density profiles of O and N under different solar EUV conditions. Fig. 4.6 shows the density profiles of O⁺, N⁺, and electrons under different solar EUV conditions. Due to more efficient dissociation of N₂ under extreme solar EUV conditions, N density can become comparable to that of O in the upper thermosphere. Interestingly, N⁺ density in the upper thermosphere (>2000 km) is always significantly smaller than that of O⁺. Only in the middle and lower thermosphere (200~1000 km) do N⁺ ions become the dominant ion species, which is probably caused by the different ion chemistry of each species.

Fig. 4.7 shows the same contents with similar parameters as those in Fig. 3.1 but under P=1500 (10x present EUV) condition. The photoionization of N is similar to that of O in the upper thermosphere because of the similar density of the corresponding atoms at high altitudes. Also in the upper thermosphere, the electron impact enhancement factor p_e/p_i reaches lower values (0.01~0.03) than that in solar minimum condition (0.04~0.2). The photodissociation and electron impact dissociation of O₂ are limited to the lower thermosphere (<200 km), similar to the situation in present Earth's thermosphere. The dissociation of N₂ occurs in a much broader altitude range (<1000 km).

5. Discussions and Summary

As discussed in last section, the dominant neutral gas heating mechanisms are the exothermic chemical reactions in the lower thermosphere and the electron collisional heating in the upper thermosphere. Both mechanisms depend on temperature (of neutral, ion, and electrons) and composition. Thus it is difficult and beyond the scope of this paper to do a complete analysis. However, it is possible to estimate how the coupling between the hydrodynamic model and the expanded GLOW model influences the energetics of the thermosphere in the model. The GLOW model computes the ionization of atomic nitrogen by electron impact, which is ignored in the parameterization, which is based on the original GLOW model. Fig. 4.7 shows that the electron impact ionization of N is greater than 1 in the lower thermosphere (<500 km) in the P=700 case. Fig. 4.6 shows that N⁺ is the dominant ion species between ~200 km and 1000 km under extreme solar EUV conditions (4.6x and 10x present EUV cases). Thus the inclusion of electron

impact ionization of N have increased the total ion and electron density in the lower thermosphere, causing more chemical and electron collisional heating of the neutral gases. In addition, the GLOW model calculates the collisions between photoelectrons and the subsequent heating of the ambient electrons explicitly. In Fig. 5.1 the two ambient electron heating rate calculated in the GLOW model is compared with that from the parameterization of Swartz and Nisbet (1972) in the P=700 case. The Swartz and Nisbet parameterization is applied by not only model I, but also the glbmean model (Roble et al. 1987, Roble 1995) and the TIE-GCM model (references). It is clear that the GLOW model provides much more heating to the ambient electrons in the upper thermosphere (>1000 km) than the parameterization in Swartz and Nisbet (1972) does under extreme solar EUV conditions. To test the model's sensitivity to the ambient electron heating treatments, we use the Swartz and Nisbet parameterization instead of the GLOW calculated values for the ambient electron heating and plot the exobase temperature as a function of solar EUV energy fluxes as a dotted curve in Fig. 4.2. It is apparent that the Swartz and Nisbet parameterization leads to significant underestimate of the exobase temperature for solar EUV energy fluxes >3x present. This suggests that the coupling of energetic electron transport model such as the GLOW model is critical in understanding the behavior of the thermosphere/ionosphere of planetary atmospheres under extreme solar EUV conditions.

To test the model's sensitivity to the adiabatic cooling in the energy equation of electron gas, we run the model without the adiabatic cooling term in the 4x and 10x present EUV cases. The model calculated exobase temperatures change from 5700 K to 5800 K (2% increase) in the 10x case and no significant difference in the 4x case. Thus adiabatic cooling does not play an important role in electron gas energy budget if electrons move at the same bulk motion velocity as neutral and ion species.

The top boundary condition for the electron gas energy equation is a fixed downward heat flux of $3e9 \text{ eV cm}^{-2} \text{ s}^{-1}$. A heat flux of comparable magnitude is required to duplicate the upper thermosphere electron temperature structure (Roble 1987, 1995, Smithtro and Sojka 2005). The source of this energy is still under debate. If we assume that this heat flux should be proportional to the incoming solar EUV energy flux, as that done in Smithtro and Sojka 2005, a heat flux of $3e10 \text{ eV cm}^{-2} \text{ s}^{-1}$ should be applied to the 10x present EUV case and this leads to a dramatic increase of the neutral gas temperature in upper thermosphere. Researches of the magnetosphere are needed in order to better constrain this boundary condition.

We note that the exobase of the Earth's atmosphere would have expanded to several Earth's radii and the plasma density could have been comparable to the neutral density. Considering the strong solar wind from a young Sun, the magnetosphere of the Earth could have been significantly more compressed billions of years ago. It is possible that the magnetospheres of early terrestrial planets shared the same space with an extended ionosphere. Nevertheless, physical processes in the magnetosphere would have been severely influenced by collisional interactions between neutral gases and plasma, similar to what's going on in the ionosphere of present Earth.

It is important to realize that the atmospheric composition of early Earth was probably different from that of today. Thus the thermospheric structure presented here is for theoretical interests only. However, with the successful coupling between a 1-D, multi-component, hydrodynamic thermospheric model and an energetic electron transport model, systematic investigations of the upper planetary atmospheres during their early evolutionary stages can be pursued on a solid ground.

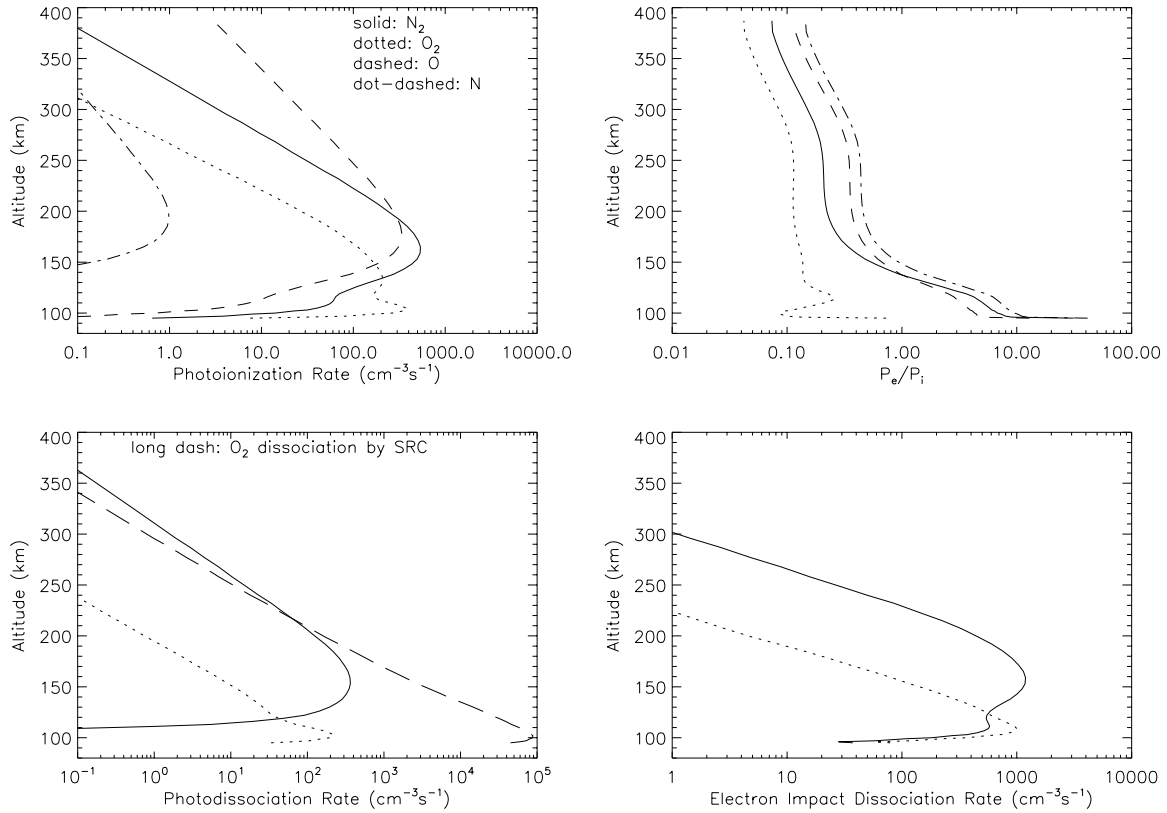


Fig. 2.1

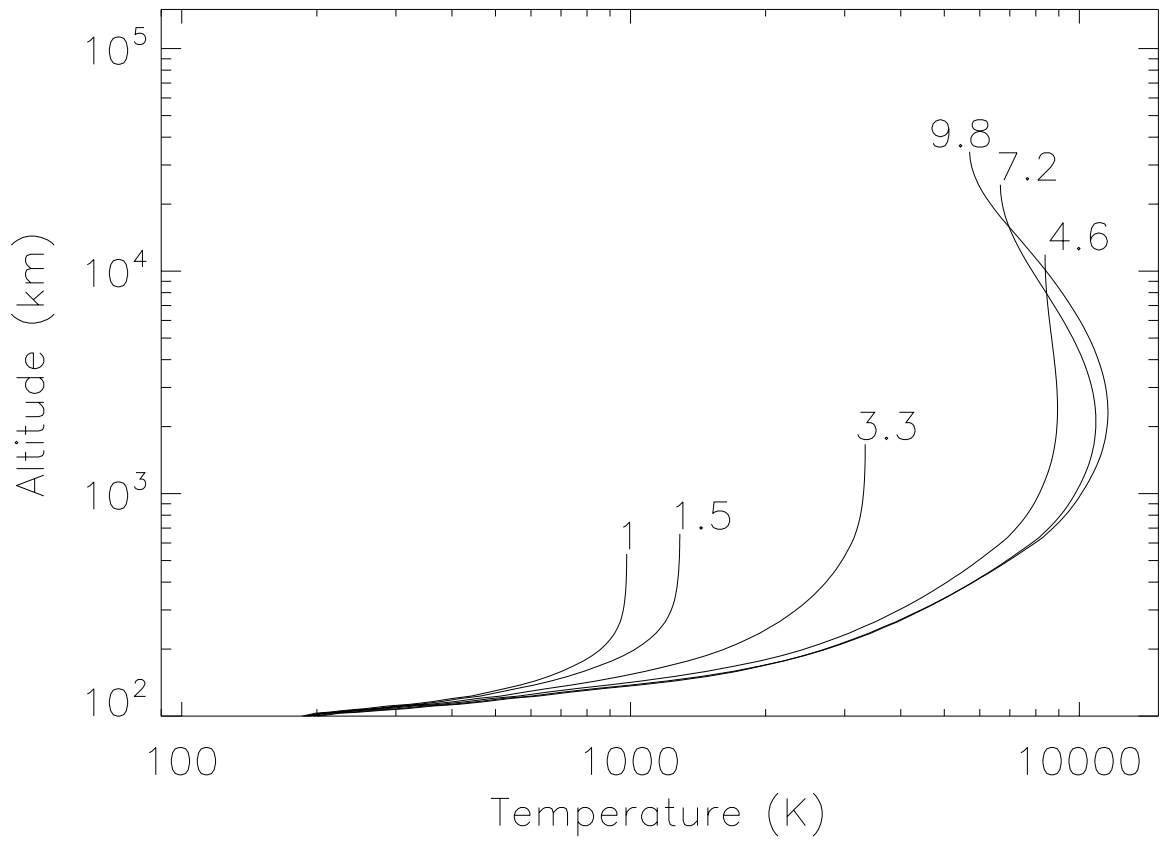


Fig. 4.1

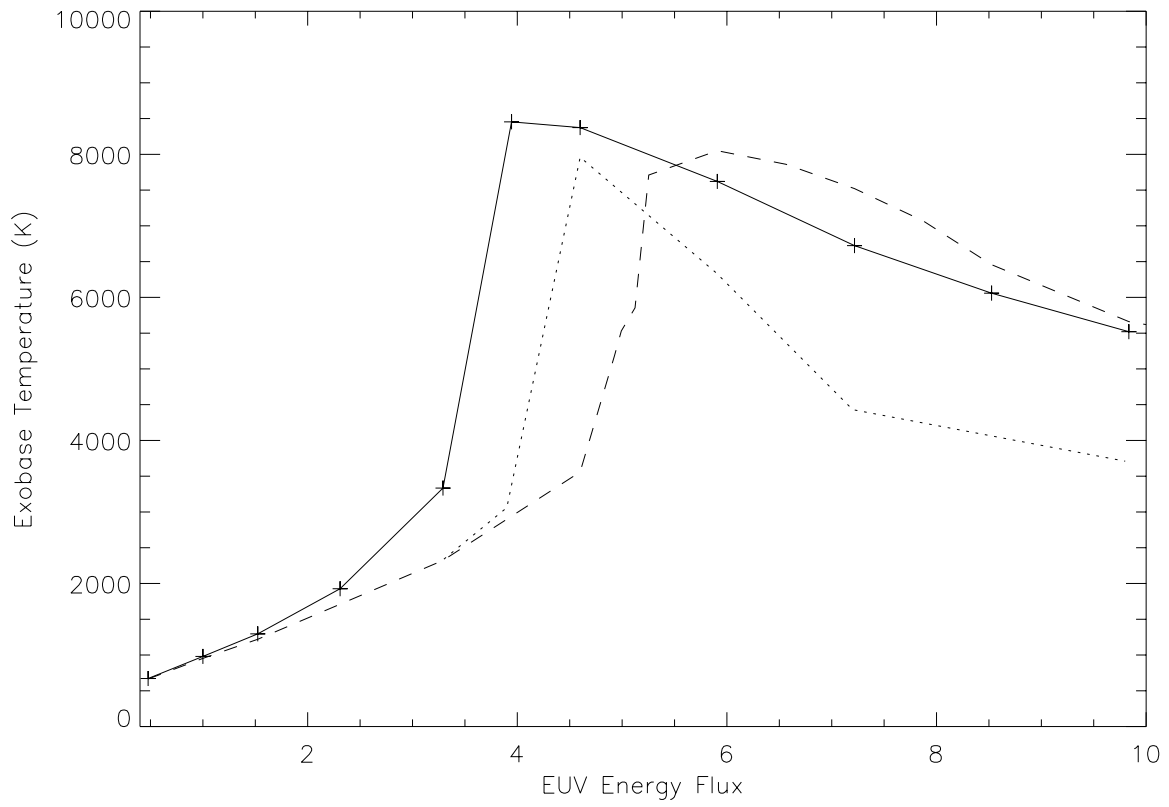


Fig. 4.2

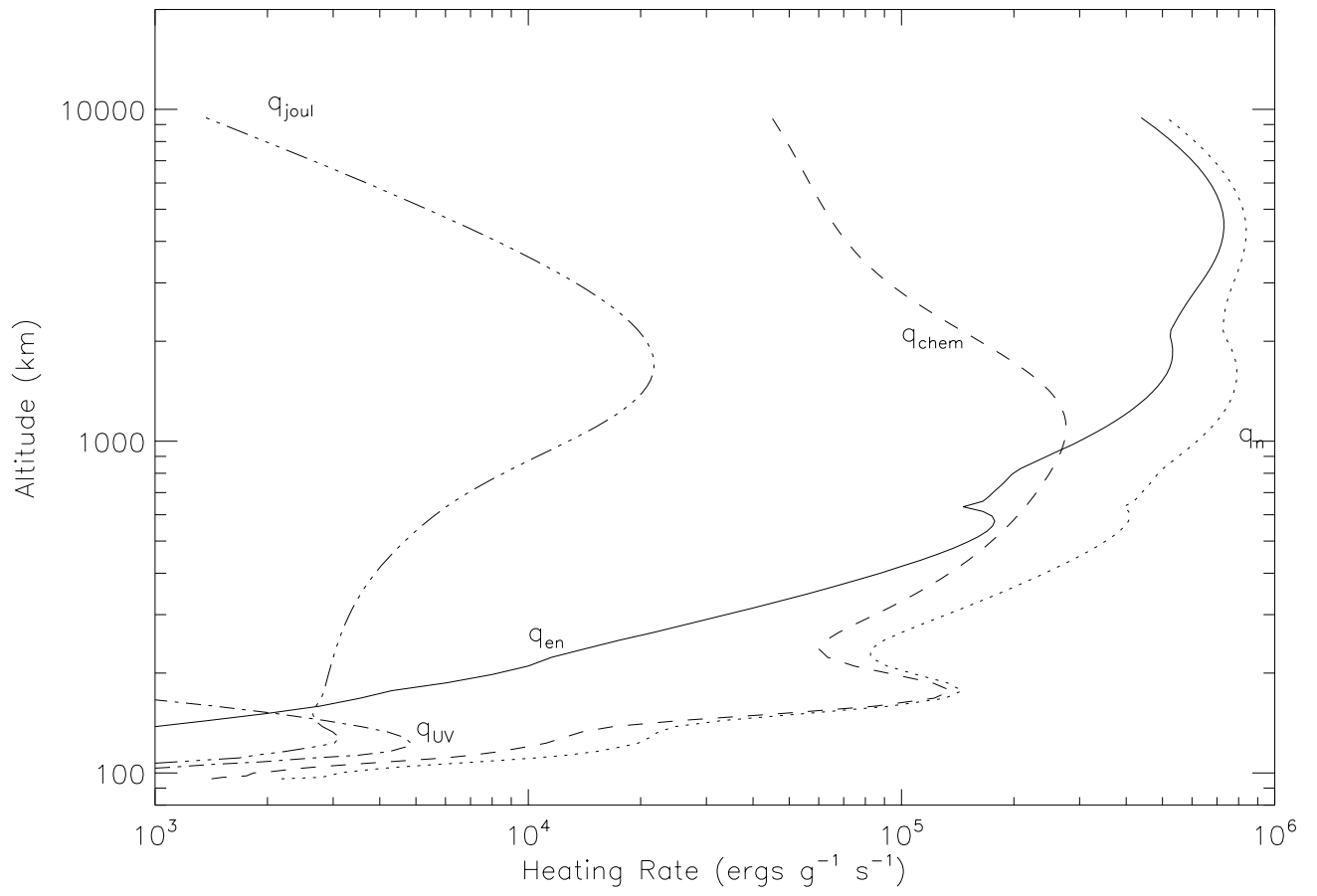


Fig. 4.3

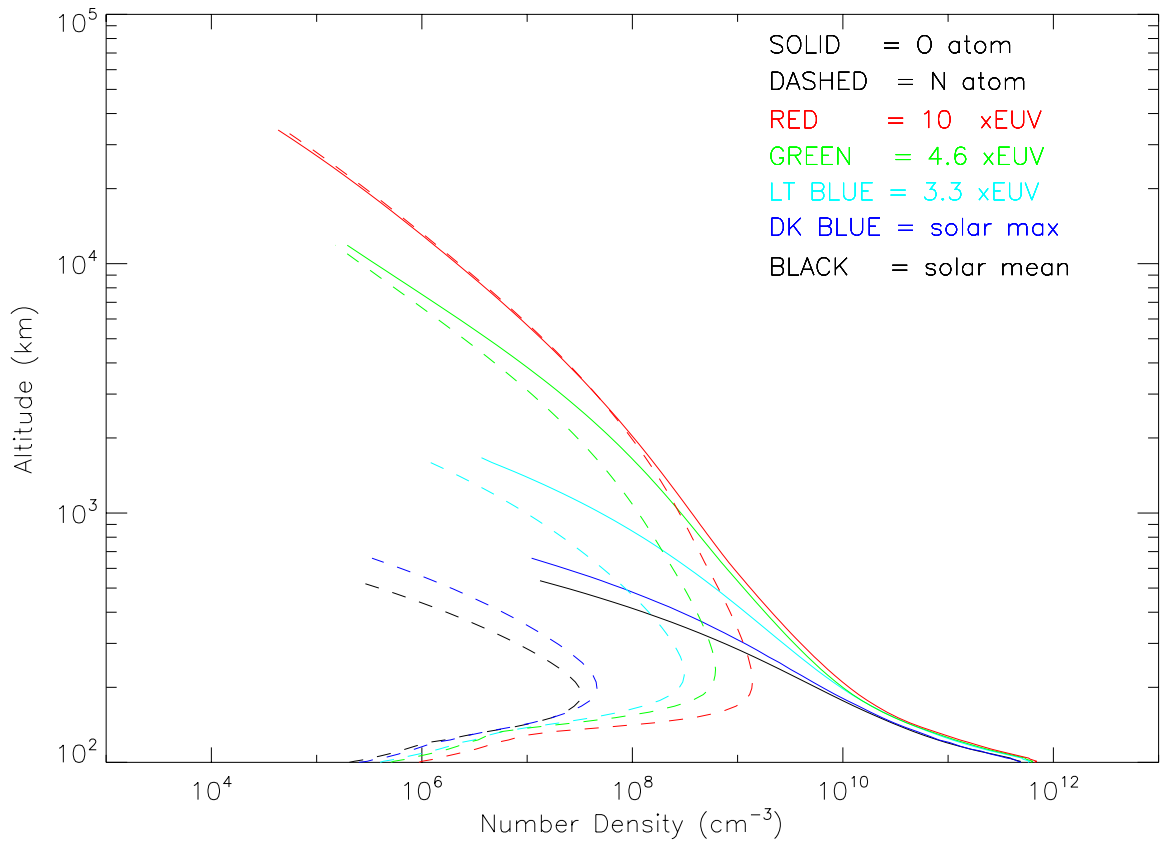


Fig. 4.5

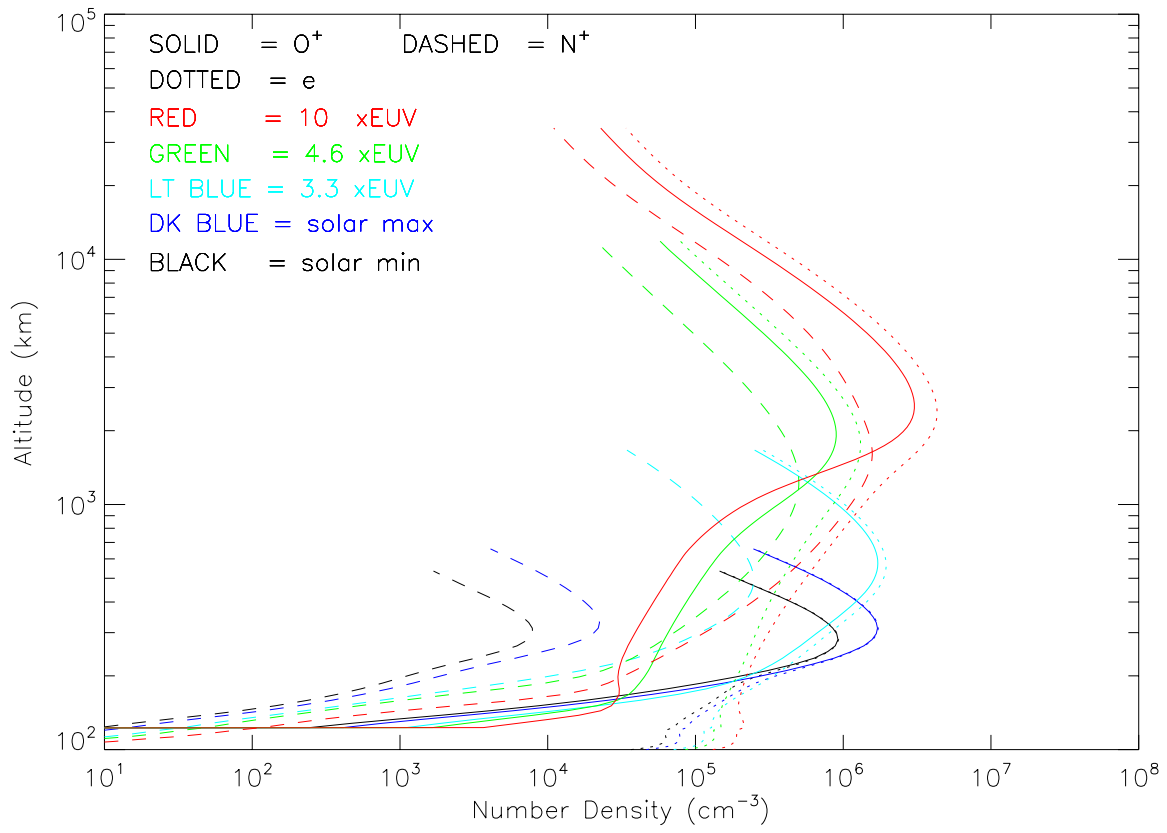


Fig. 4.6

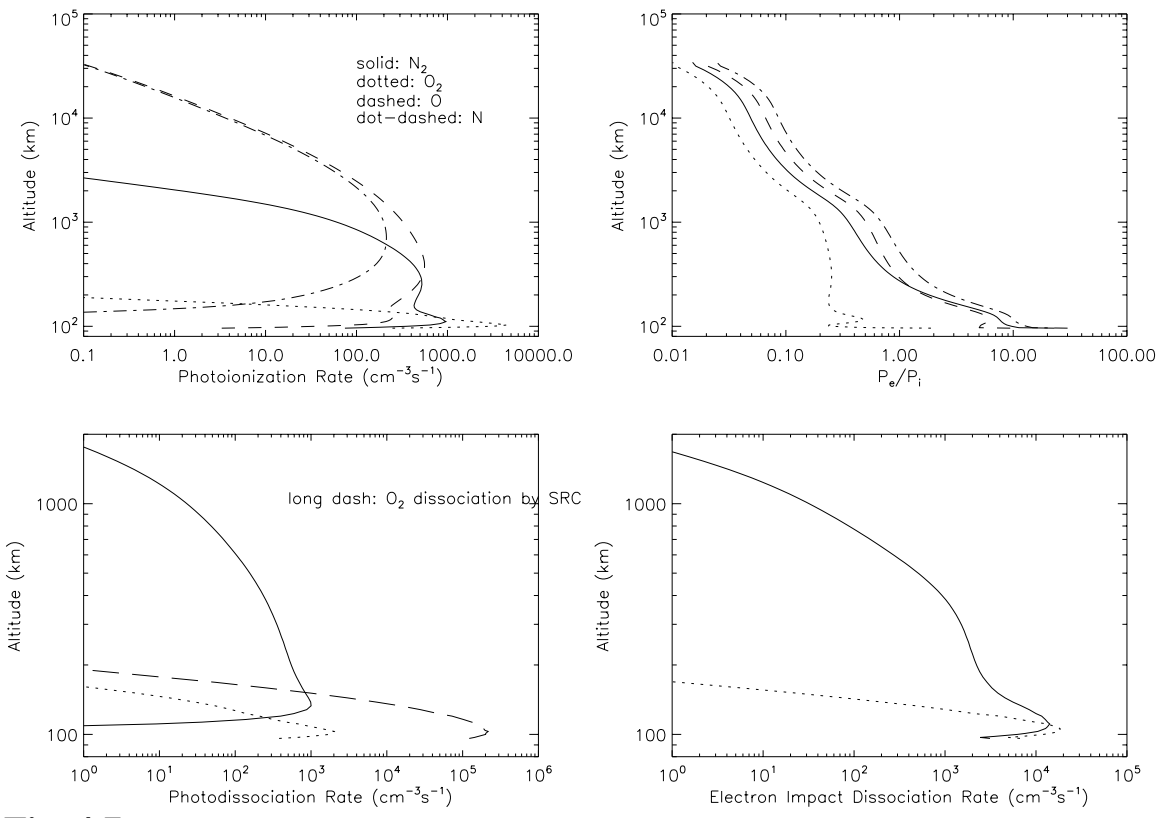


Fig. 4.7

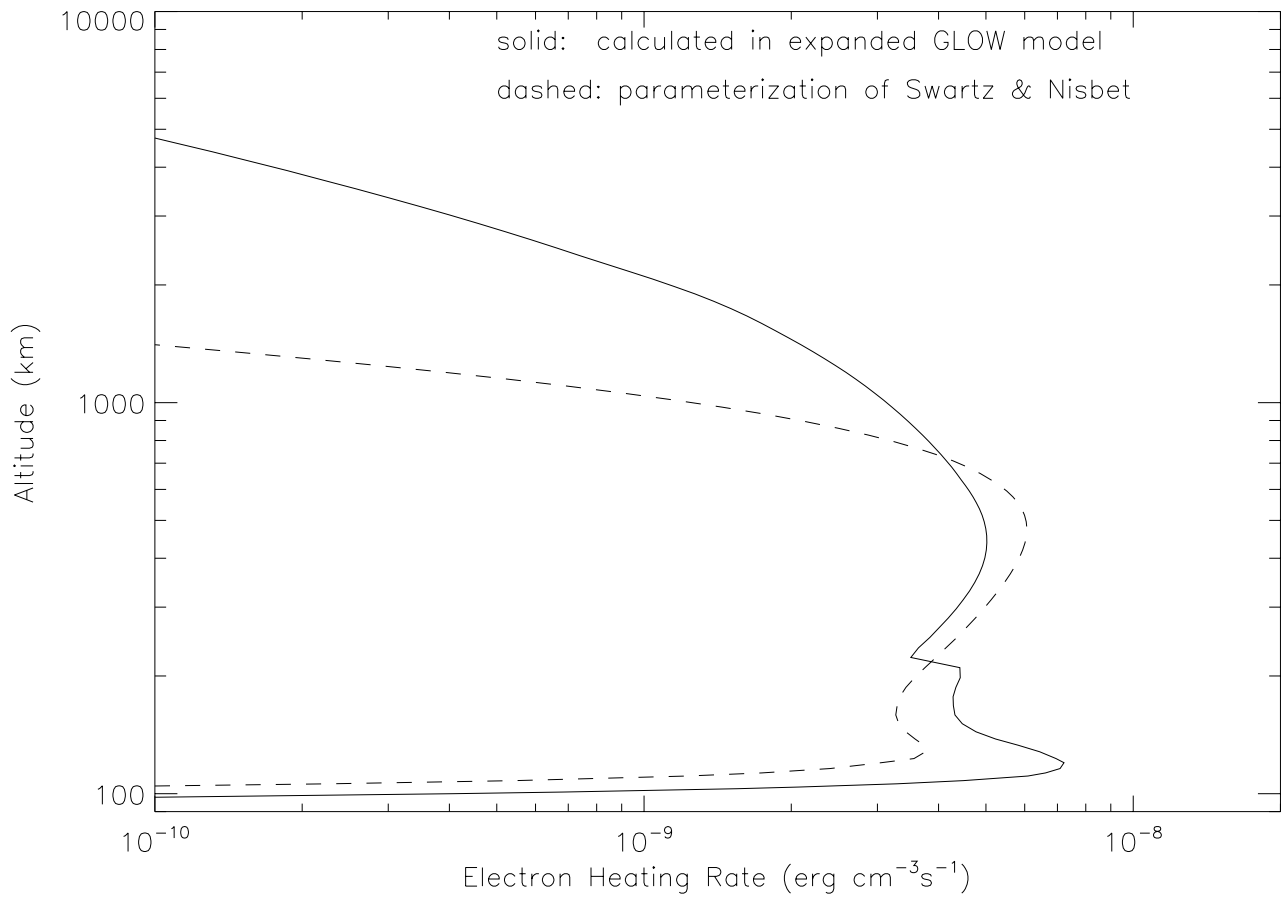


Fig. 5.1

References (incomplete):

Alexander, M. J., A. I. F. Stewart, S. C. Solomon, and S. W. Bougher. Local-time asymmetries in the Venus thermosphere. *J. Geophys. Res.*, **98**, 10849, 1993.

Avakyan, S. V., et al. 1998, Collision Processes and Excitation of UV Emission from Planetary Atmospheric Gases (Amsterdam: Gordon & Breach)

Bailey, S. M., C. A. Barth, and S.C. Solomon. A model of nitric oxide in the lower thermosphere. *J. Geophys. Res.*, **107**, 1205, doi:10.1029/2001JA000258, 2002.

Fennelly, J.A., and D.G. Torr (1992) Photoionization and photoabsorption cross sections of O, N₂, O₂, and N for aeronomic calculations. *At. Data and Nucl. Data Tables* 51, 321

Hintereger, H.E., K. Fukui, and G.R. Gilson (1981) Observational, reference, and model data on solar EUV, from measurements on AE-E. *GRL* 8, 1147

Jackman, C.H., R.H. Garvey, and A.E.S. Green (1977) Electron impact on atmospheric gases I. Updated cross sections. *J.G.R.* 82, 5081

Green, A.E.S. and R.S. Stolarski (1972) Analytic models of electron impact excitation cross sections. *J. Atmospheric and Terrestrial Physics* 34, 1703

Green, A.E.S. and T. Sawada (1972) Ionization cross sections and secondary electron distributions. *J. Atmospheric and Terrestrial Physics* 34, 1719

Meier, R. R. (1991) *Space Sci. Rev.* **58**, 1

Nay, A.F., and P.M. Banks (1970) Photoelectron fluxes in the ionosphere. *J. Geophys. Res.*, 75, 6260

Schunk, R. W., and A. F. Nagy (2000), *Ionospheres: Physics, Plasma Physics, and Chemistry*, Cambridge Univ. Press, New York.

Stolarski, R.S., P.B. Hays, and R.G. Roble (1975) Atmospheric heating by solar EUV radiation. *JGR* 80, 2266

Stolarski, R.S. (1976) Energetics of the midlatitude thermosphere. *J. Atmospheric and Terrestrial Physics* 38, 863

Solomon, S. C., P. B. Hays, and V. J. Abreu, The auroral 6300Å emission: Observations and modeling, *J. Geophys. Res.*, 93, 9867, 1988.

Solomon, S. C., and V. J. Abreu. The 630 nm dayglow. *J. Geophys. Res.*, **94**, 6817, 1989.

Solomon, S. C. and L. Qian, Solar extreme-ultraviolet irradiance for general circulation models, *J. Geophys. Res.*, 110, A10306, doi:10.1029/2005JA011160, 2005.

Stone, E.J., and E.C. Zipf (1973) Excitation of atomic nitrogen by electron impact. *The Journal of Chemical Physics* 58, 4278

Swartz, W.E., and J.S. Nosbet (1972) Revised calculations of F region ambient electron heating by photoelectrons. *J.G.R.* 77, 6259

Tayal, S.S., and O. Zatsarinny (2005) B-spline R-matrix with pseudostates approach for electron impact excitation of atomic nitrogen. *J. Phys. B: At. Mol. Opt. Phys.* 38, 3631

Zipf, E.C., and P.W. Erdman (1985) Electron impact excitation of atomic oxygen: revised cross sections. *J.G.R.* 90, 11087

